Available online at www.sciencedirect.com
SCIENCE DIRECT®
Ocean Modelling 11 (2006) 193–213
Ocean Modelling
www.elsevier.com/locate/ocemod

Influence of the wind waves dissipation processes on dynamics in the water upper layer

V.G. Polnikov [a,*], P. Tkalich [b]

[a] *Air–Sea Interaction Laboratory, A.M. Obukhov Institute for Physics of Atmosphere of the Russian Academy of Sciences, Pyzhevskii Lane 3, 119017 Moscow, Russia*
[b] *Tropical Marine Science Institute, National University of Singapore, Singapore 119223, Singapore*

Received 20 September 2004; received in revised form 9 December 2004; accepted 20 December 2004
Available online 24 January 2005

Abstract

Stochastic surface wind waves are considered as an intermediate physical phenomenon responsible for the state of upper layer of the water column. Mathematical formulation of the problem is done by using the wind wave spectral evolution model. It is shown that parameters of the air boundary layer are controlled by input evolution mechanism of wind waves, while dissipation mechanism is important for description of energy and momentum transfer into upper layer of the water column. Estimations of the wave energy dissipation rate are found utilizing the optimized numerical model for wind waves derived earlier. Such estimations can be used for better description of numerous important phenomena at the air–sea surface, including air bubbles entrainment, vertical mixing of oil slicks, near surface shear flow and many others. Three applications of the theory are presented.

Keywords: Wind waves; Numerical model; Wave spectrum; Energy and momentum flux; Air boundary layer; Turbulent energy

* Corresponding author. Tel.: +7 095 9518549; fax: +7 095 9531652.
E-mail addresses: polnikov@mail.ru (V.G. Polnikov), tmspt@nus.edu.sg (P. Tkalich).

1463-5003/$ - see front matter © 2005 Elsevier Ltd. All rights reserved.
doi:10.1016/j.ocemod.2004.12.006

1. Introduction

Let us consider a typical air–sea interface, including three major phenomena (Fig. 1):

- Turbulent air boundary layer with the shear mean wind having a velocity value $\mathbf{W}_{10}(\mathbf{x})$ at the level 10 m above the surface.
- Water wavy surface.
- Thin water upper layer with turbulent motions and mean shear currents.

Mean wind blowing above the surface is one of the major sources of mechanical motions at the air–sea interface. Typical temporal and spatial scales of winds may vary within thousand meters and thousand seconds. The same time, variability of the wavy surface has scales of tens meters and ten seconds. Thus wind impacts the upper layer of water column indirectly via the middle scale motions of wind waves. This impact is transferred further in to the upper water layer motions having a wide range of scales.

Keeping in mind numerous potential applications, it is important to describe in a physically-sound concise mathematical form the interaction between major phenomena, responsible for exchange processes at the air–sea interface. Implementation of the model would allow improvement of wave and current forecast, calculation of mass and heat exchange between atmosphere and ocean, pollution mixing, and many other applications.

Direct mathematical description of the considered problem is very complex due to interplay of several multiple-scale stochastic phenomena. As it was pointed out by Kitaigorodskii and Lumley (1983), such description can not be done in an exact form. Nevertheless, considerable advantage can be achieved using spectral representation of wave dynamics. Up-to-date, a principal physical understanding of exchange processes at the air–sea interface was achieved to some extent (Donelan, 1994; Banner, 1999), and mathematical tools for their description in spectral representation have been constructed (as in Phillips, 1977). A short review in the next section summarizes the major findings.

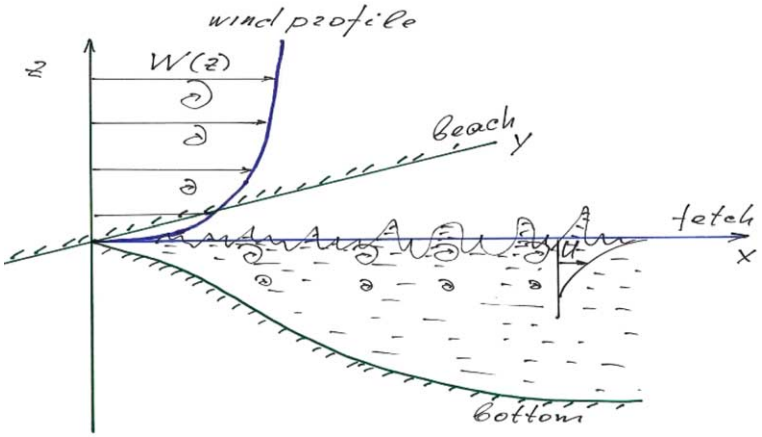

Fig. 1. The air–sea interface system.

2. Problem formulation

Due to a turbulent nature, small scale motions at the sea surface interface are generated very quickly. These motions, having scale less than one meter and one second, are relevant to the background near-wall turbulence (taking place both, in the air boundary and water's upper layer). Mechanism of energy flux from the mean wind to the wave motion initiation was described in a spectral form by Phillips (1957). The same time, Miles (1957) have shown that at the following stage of wave evolution, the Phillips' mechanism is replaced by more intensive feedback mechanism. Since than, both mechanisms were elaborated further by numerous authors (see Phillips, 1977), but the problem of energy flux from wind to waves has not been solved in a consistent form. Until now the both mechanisms are used in a simplified form using experimental observations (Komen et al., 1994).

During initial period of several hours the small scale motions of the wavy surface are transformed in to the middle scale motions (known as the wind waves) ranging from turbulent ones to the order of several tens meters and ten seconds. Wind waves grow due to conservative nonlinear interactions among a wave continuum (Hasselmann, 1962), backed by the energy supply mechanism of Miles (1957).

As a feedback, waves affect the air boundary layer turbulence, which becomes much more intensive than the initial near-wall turbulence. Moreover, evolving waves impact air boundary layer, changing parameters of turbulent fluxes and mean wind profile. This feedback mechanism has being investigated recently by Makin and Kudryavtsev (1999) within the so-called theory of dynamic boundary layer. It was shown that the well known great variability of boundary layer parameters (such as the drag coefficient C_d, roughness length z_0, and others) can be described using the dynamic boundary layer theory (Polnikov et al., 2003). Hence, one can say that the feedback mechanism model is already constructed in a spectral form, so that there is a possibility to focus on other evolution mechanisms. Due to the wave instability and breaking, the lost energy is generating turbulence in upper layer of the water column. These intensive small scale motions are important in many applications dealing with air bubbles entrainment, vertical mixing of admixtures, heat and gas exchange, and many others (for some references see Tkalich and Chan, 2002a; Qiao et al., 2004). Some part of the dissipated wave energy and momentum can be expended to generate large scale motions (currents). Thus, wind wave dissipation may affect state of the entire water column.

It is clear that wind waves play a mediation role in atmosphere–ocean interactions at different temporal and spatial scales. Even though, mathematical model of wind–wave interactions at the air boundary layer is more or less developed, description of wave–turbulence interactions in upper layer of the water column is less formalized. The latter topic is the major focus of this paper.

It is well known that the motion intensity of any scale in the upper layer of water column, I_{upp}, depends directly on intensity of near-surface turbulence motion, I_{turb}, located in a thin upper layer having thickness comparable with the mean wave height. But the wave dissipation processes are the major contributor of energy into the near-surface turbulence, and the rate of this contribution can be denoted as D_E. A certain part of this wave energy dissipation rate is the rate of turbulent energy production in the water upper layer, E_{turb}. Thus, the energy cascade in the upper layer can be schematically expressed in the form

$$I_{upp} \propto I_{turb} \propto E_{turb} \propto D_E. \tag{1}$$

This relationship is used in theoretical estimations of small scale phenomena in the mixing layer (such as Tkalich and Chan, 2002a,b; Qiao et al., 2004). Production of mechanical motions in the thin water layer can theoretically be described using a spectral approach to the wind wave dissipation phenomenon. Since, the latter is strongly related to other wave evolution mechanisms, one needs to consider the complete wind wave model in a spectral form.

Latest generation of wind wave models use wave action spectrum of the surface elevation, $N(\mathbf{k})$, represented in a spectral space of the wave vector, $\mathbf{k}$ (Komen et al., 1994; Tolman and Chalikov, 1996). But in practice it is preferable to use frequency-angular form of the energy spectrum $S(\sigma,\theta,\mathbf{x},t)$, shortly noted as S. For deep water case without ambient currents, wind wave evolution equation has a form of transport equation for the spectrum S:

$$\frac{\partial S}{\partial t}+C_{\mathrm{g}x}\frac{\partial S}{\partial x}+C_{\mathrm{g}y}\frac{\partial S}{\partial y}=F(\mathbf{W},S)\equiv In(\mathbf{W},S)-Dis(\mathbf{W},S)+Nl(S). \tag{2}$$

Here $\mathbf{C}_{\mathrm{g}}=(C_{\mathrm{g}x},C_{\mathrm{g}y})=\frac{\partial\sigma(k)}{\partial k}\frac{\mathbf{k}}{k}$ is the group velocity vector for the wave component with frequency $\sigma(k)$ and direction θ, corresponding to the polar co-ordinate form of the wave vector $\mathbf{k}=(k,\theta)$, and F is the so-called source function written for the energy wave spectrum $S(\sigma,\theta)$ in the frequency-angle form.[1] In the deep water case, the energy spectrum $S(\sigma,\theta)$ is related to the wave action spectrum $N(\mathbf{k})$ as

$$S(\sigma,\theta)=\frac{\sigma}{4\pi^2 g}N(\sigma,\theta)=\frac{\sigma}{4\pi^2 g}\frac{k}{C_{\mathrm{g}}}N(\mathbf{k}). \tag{3}$$

The term F in the left part of Eq. (2) is the total rate of spectral wave energy change, which include three main evolution mechanisms expressed in terms of the local wind $\mathbf{W}(\mathbf{x},t)$, wave parameters σ and θ, and wave spectrum $S(\sigma,\theta)$. They are as follows:[2]

- $In[\mathbf{W},\sigma,\theta,S(\sigma,\theta)]$ is the rate of wave energy input due to wind $\mathbf{W}(\mathbf{x},t)$ (the input term);
- $Dis[\mathbf{W},\sigma,\theta,S(\sigma,\theta)]$ is the rate of wave energy dissipation (the dissipation term);
- $Nl[S(\sigma,\theta),\sigma,\theta]$ is the rate of conservative nonlinear energy transfer through the spectrum due to wave–wave interaction mechanism independent of wind (the nonlinear term).

Once Eq. (2) is solved in the (σ,θ)-space, the wave momentum spectral density, $\mathbf{M}(\sigma,\theta)$, can be calculated as

$$\mathbf{M}(\sigma,\theta)=\mathbf{k}N(\sigma,\theta)=4\pi^2 g\frac{\mathbf{k}}{\sigma}S(\sigma,\theta). \tag{4}$$

The wave evolution mechanisms are discussed widely in the literature (for references, see Komen et al., 1994; Efimov and Polnikov, 1991; Tolman and Chalikov, 1996). It is widely recognized that the nonlinear mechanism of wave evolution is the most theoretically addressed, while the input mechanism is more experimentally studied, and the dissipation mechanism is the least investigated. Moreover, role of the latter mechanism is not well discussed in the literature and the wave

[1] Relationship between frequency σ and wave number k is given by the well known dispersion equation for surface waves.

[2] Hereafter some arguments in functions used would be omitted for the notation simplicity.

research community. The main aim of this paper is to show the principal role of wind waves (as a phenomenon), and the dissipation processes, in particular, in the entire momentum and energy budget at the air–sea interface. Another aim is to demonstrate practical applications of the dissipation rate quantification during the wave evolution.

To cover the topic, basic scheme of energy budget at the air–sea interface is reproduced in the Section 3. Section 4 considers all wave evolution terms, with main attention paid to the dissipation mechanism. In Section 5 some numerical estimations of the wave energy dissipation into the upper layer are calculated for two typical scenarios. Section 6 considers application of the theory for quantification of air bubbles and oil droplets entrainment into the mixing layer; additionally, some other possible applications are discussed.

3. Energy budget at the air–sea interface

Local wind with velocity $\mathbf{W}(\mathbf{x}, t)$ can be characterized by the local surface density of the wind energy flux as (Kitaigorodskii and Lumley, 1983),

$$\mathbf{F}_{\mathrm{WE}} = \rho_{\mathrm{a}} W^2 \mathbf{W}/2, \tag{5}$$

and by the local surface density of the wind momentum flux,

$$\mathbf{F}_{\mathrm{WM}} = \rho_{\mathrm{a}} W \mathbf{W}, \tag{6}$$

where ρ_{a} is the air density, and W is the modulus of the wind vector. Both these fluxes are corresponding to the one unit height of the air column above the water. One part of this energy is spent to the wind wave motions, and another part is transferred to the upper layer of the water column, resulting in the water mass motions of different space–time scales. A simplified scheme of the wind energy flux budget is considered below.

Definition for the vertical flux of horizontal wind momentum (per unit time of unit area) is

$$\tau(z) = -\rho_{\mathrm{a}} \langle u' w' \rangle. \tag{7}$$

Here, u' and w' are the turbulent fluctuations of horizontal and vertical velocities of the boundary air flow at level z above the mean water surface. The entire momentum is transferred into the water surface and the water upper layer motions due to the boundary layer turbulence mechanism, which is similar to the near-wall turbulence (Monin and Yaglom, 1965). This momentum flux can be quantified using the so-called friction velocity, u_*, as

$$\tau = \rho_{\mathrm{a}} u_*^2 = \rho_{\mathrm{a}} C_{\mathrm{d}} W^2, \tag{8}$$

where C_{d} is the drag coefficient having order of $(1\text{–}3)10^{-3}$. In general, this value depends on the stage of wave evolution (i.e., on the wave spectrum S) and other ambient parameters.

It is important to note that the wind stress is nearly constant in vertical direction for the steady vertical wind profile (Chalikov and Belevich, 1993). For the air–sea interface the total wind stress, τ, can be represented as the sum of purely turbulent part, τ_{t}, (corresponding to the hard-wall turbulence) and wave induced one, τ_{w}. Thus, neglecting relatively small viscosity part of the total stress, one obtains

$$\tau = \tau_{\mathrm{t}} + \tau_{\mathrm{w}} = \mathrm{const}. \tag{9}$$

In some cases, particular theory of wind vertical profile can be constructed (as in Makin and Kudryavtsev, 1999), and explicit relationship between τ_t and τ_w can be established, reducing number of unknowns to τ_w only. Generally, near the wavy surface the following relationship is valid

$$\tau_w \geqslant \tau_t. \tag{10}$$

At any spatial point, the momentum flux $\vec{\tau}_w$ is directly related to the wave spectrum $S(\sigma,\theta)$ via the input term of the source function, $In(\mathbf{W},S)$, as (in Makin and Kudryavtsev, 1999)

$$\vec{\tau}_w(z) = \rho_w g \int_0^\infty d\sigma \int_0^{2\pi} d\theta \frac{\mathbf{k}}{\sigma} \Phi(k,z) In[\mathbf{W}, S(\sigma,\theta)], \tag{11}$$

where ρ_w is the water density, g is the gravity acceleration, and $\Phi(k,z)$ is the known vertical structure function. General expression for the total energy flux from wind to waves (per unit time of unit area) assumes the form

$$I_E = \rho_w g \int_0^\infty d\sigma \int_0^{2\pi} d\theta In[\mathbf{W}, S(\sigma,\theta)], \tag{12}$$

where the boundary condition $\Phi(k,0) = 1$ is used. In other words, expression (12) defines the rate of energy input from wind to waves, I_E.[3]

These expressions suggest that in addition to the local wind, $\mathbf{W}(\mathbf{x},t)$, the local state of wave field defines the rate of momentum and energy input into the upper layer, depending on the shape of local two-dimensional wave spectrum $S(\sigma,\theta)$. Numerical estimations of these both inputs follow from solution of the evolution equation (2) with chosen terms of the source function F and using relationships (11) or (12). It is clear that all wind waves evolution mechanisms play an important role in energy and moment exchange at the air–sea interface. But the question remains on what part of wave energy is transferred into the upper layer of the water column? To answer this question one has to quantify the entire scheme of energy and momentum distribution at the air–sea interface.

Total wave energy per unit area, E, at the fixed space–time location $(\mathbf{x},t)$ is given by

$$E(\mathbf{x},t) = \rho_w g \int_0^\infty d\sigma \int_0^{2\pi} d\theta S(\sigma,\theta,\mathbf{x},t). \tag{13}$$

Note, that wave energy often is measured in units of length squared. In this case, the multiplicand $\rho_w g$ is omitted in formula (13), and consequently in Eqs. (11) and (12). Further in this paper, the complete unit of wave energy is used.

We remind that accumulation of the total wave energy is provided not only by the input evolution mechanism, but also by means of all evolution mechanisms for wind waves. Some part of the gained local wave energy is transferred into the water upper layer. This part is governed by the dissipation term of the source function F. The rate of wave energy dissipation per unit time and area, D_E is given by the expression

[3] Of course, here we do not take into account a frictional feedback of breaking processes on the atmosphere boundary layer. This question needs more complicated consideration.

$$D_{\mathrm{E}}(x,t) = \rho_{\mathrm{w}} g \int_0^{\infty} \mathrm{d}\sigma \int_0^{2\pi} \mathrm{d}\theta Dis[\mathbf{W}, S(\sigma,\theta,x,t)]. \tag{14}$$

Thus, a detailed numerical description of the dissipation term *Dis* (**W**, *S*) is needed to calculate the rate of wave energy dissipation. But the latter magnitude depends strongly on the wind **W**, and the shape and intensity of the wave spectrum *S*. To quantify the magnitude of D_{E} adequately, one needs to introduce new dimensionless magnitude, the relative dissipation rate, D_{RE}, defined as

$$D_{\mathrm{RE}} = D_{\mathrm{E}}/Ef_{\mathrm{p}}, \tag{15}$$

where f_{p} is the peak frequency given in Hz ($f_{\mathrm{p}} = 2\pi\sigma_{\mathrm{p}}$). Value D_{RE} quantifies relative part of wave energy dissipated at mean wave period, *T*. Thus, simultaneous calculation of the total wave energy *E*, peak frequency f_{p} and D_{E} allows tabulate D_{RE} as a function of wind and spectral shape. In this approach, estimation of the mentioned earlier rate of upper turbulence production, E_{turb}, is given by the expression

$$E_{\mathrm{turb}} \equiv c_{\mathrm{d}} D_{\mathrm{E}} = c_{\mathrm{d}} D_{\mathrm{RE}} Ef_{\mathrm{p}}, \tag{16}$$

where c_{d} is the coefficient depending on the type of turbulent (or mixing) process considered in the upper layer of the water column.

The non-dimensional value D_{RE} can be estimated and tabulated for typical scenarios of wave evolution. Expression (16) conveniently links such integral wave parameters as energy *E* and peak frequency f_{p}, to tabulated non-dimensional value D_{RE}. Since coefficient c_{d} is known, the dissipation rate E_{dis} can be quantified for typical applications. Some examples of the estimation is given in Section 6. Finalizing the section it is important to stress that the dissipated energy is shared into two parts. One part is transferred into motions having certain mean momentum, such as surface currents with velocity $U(\mathbf{x})$ and the surface density of kinetic energy per unit volume, $E_{\mathrm{C}}=\rho_{\mathrm{w}}U^2/2$. Another part of the wave energy is transferred to momentumless motions. This part generates turbulence in the upper layer with the surface density of kinetic energy, E_{T}. Exact amount of energy in each part is not known a priori, but it can be estimated theoretically using conservation laws and proper large scale circulation model (Pedlosky, 1982). Rough estimation can be given by the following ratio (Makin and Kudryavtsev, 1999)

$$\frac{E_{\mathrm{C}}}{E_{\mathrm{T}}} \cong \frac{\tau_{\mathrm{t}}}{\tau_{\mathrm{w}}} \approx 0.3\text{–}0.5. \tag{17}$$

Turbulent motion energy is expended mainly for initiation and support of vertical mixture processes. These processes are related, for example, to air bubble entrainment, gas and heat exchange, water temperature and salinity stratification in the upper layer of the water column. This part of energy works against buoyancy forces. Some description of such processes can be found in papers of Tkalich and Chan (2002a,b) or Qiao et al. (2004) and in references cited there. Each application requires separate quantitative estimation of energy and momentum budget. General scheme of energy redistribution at the air–sea interface is illustrated in Fig. 2. It is clear that this budget is mainly defined by evolution mechanisms of wind waves. Therefore, a rigorous numerical description of these mechanisms should be done as accurate as possible, similar to analysis suggested in the next section.

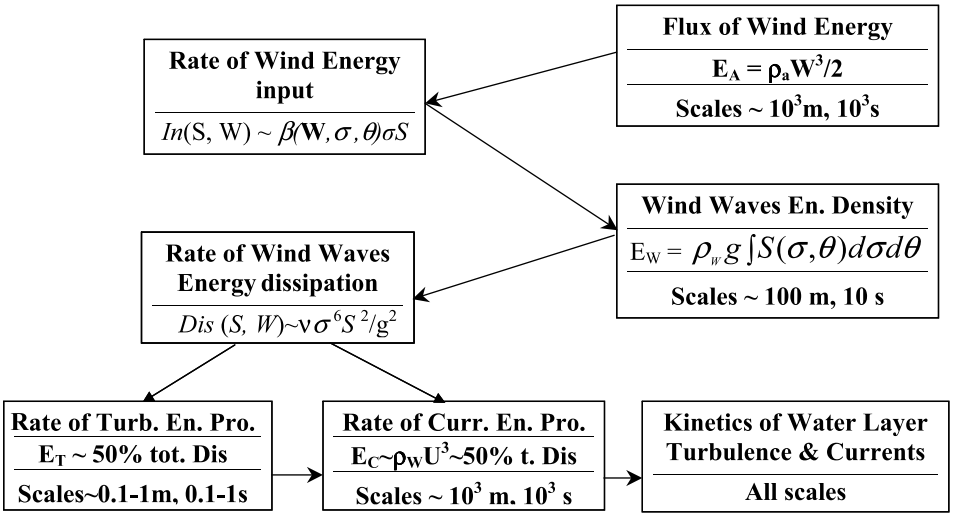

Fig. 2. Scheme of the energy flux distribution at the air–sea interface.

4. Source terms formulation

We start with a brief analysis of the nonlinear mechanism of wave evolution (*Nl*-term) which is the best theoretically investigated in the literature. Then, a semi-empirical parameterization of the input term (*In*) follows, along with description of dynamic boundary layer using theoretical model of Makin and Kudryavtsev (1999). Since, the dissipation mechanism (*Dis*-term) is the least theoretically understood, we provide in-depth analysis of the parameterization following Polnikov (2005).

4.1. Nl-term

Well known Discrete Interaction Approximation—DIA (Hasselmann et al., 1985) is used for parameterization of *Nl*-term. Having optimal ratio of accuracy versus computation efficiency, DIA is the most effective parameterization of *Nl*-term (Polnikov and Farina, 2002). In present paper the modified version of DIA (fast DIA) is used (Polnikov, 2003). The frequency-angle numerical grid, $\{\sigma_i, \theta_j\}$, is given by expressions

$$\sigma_i = \sigma_{\text{low}} \cdot \mu^{i-1} \quad (0 \leqslant i \leqslant I), \tag{18}$$

$$\theta_j = -\pi + j\Delta\theta \quad (1 \leqslant j \leqslant J), \tag{19}$$

where σ_{low} is the lowest frequency under consideration, μ and $\Delta\theta = 2\pi/J$ are the grid resolution parameters, I is the number of frequencies, and J is the number of angles;

$$\mu = 1.05, \quad I = 40, \quad \text{and} \quad J = 36\ (\Delta\theta = 10^\circ). \tag{20}$$

The choice of value σ_{low} does not influence the parameterization, though it defines the frequency interval under consideration. One configuration of four interacting waves in the used version of DIA is given by expressions

$$\sigma_1 = \sigma\mu^4, \quad \sigma_2 = \sigma\mu^5, \quad \sigma_3 = \sigma\mu^8, \tag{21}$$

and

$$\theta_1 = \theta + 2\Delta\theta, \quad \theta_2 = \theta + 2\Delta\theta, \quad \theta_3 = \theta + 3\Delta\theta. \tag{22}$$

with current values for σ and θ, for which a loop is organized in accordance with the typical DIA procedure. In such a case, one has

$$Nl(\sigma,\theta) = I(\sigma_1,\theta_1,\sigma_2,\theta_2,\sigma_3,\theta_3,\sigma,\theta), \tag{23}$$

where

$$I(\sigma_1,\theta_1,\sigma_2,\theta_2,\sigma_3,\theta_3,\sigma,\theta) = C\sigma^{11}[S_1S_2(S_3 + (\sigma_3/\sigma)^4 S) - S_3S((\sigma_2/\sigma)^4 S_1 + (\sigma_1/\sigma)^4 S_2)], \tag{24}$$

and $S_i = S(\sigma_i,\theta_i)$. The fitting constant C in (24) is found to be 12 000. Due to conservativeness of nonlinear gravity waves, the following expressions are used in the loop for σ and θ:

$$Nl(\sigma_3,\theta_3) = Nl(\sigma,\theta), \quad Nl(\sigma_1,\theta_1) = Nl(\sigma_2,\theta_2) = -Nl(\sigma,\theta). \tag{25}$$

Finally, it results in the energy conservation expression

$$\int_0^\infty \mathrm{d}\sigma \int_0^{2\pi} \mathrm{d}\theta Nl(\sigma,\theta) \equiv 0. \tag{26}$$

4.1.1. In-term

For *In*-term, widely recognized Miles' (1957) model is used

$$In = \beta(\sigma,\theta,\mathbf{W})\sigma S(\sigma,\theta). \tag{27}$$

Here the growing parameter, $\beta(\sigma,\theta,\mathbf{W})$ for the wind direction angle, θ_w, is parameterized as

$$\beta = \max\left\{-b_L, \left[0.04\left(\frac{u_*\sigma}{g}\right)^2 + 0.00544\frac{u_*\sigma}{g} + 0.000055\right]\cos(\theta - \theta_w) - 0.00031\right\} \tag{28}$$

with the limiting value $b_L = 5\times10^{-6}$. This form uses empirical data of Snyder et al. (1981), Plant (1982), and generalization of Yan (1987); as well as theoretical work of Chalikov (1980), who introduced limiting coefficient β for waves running faster than the local wind W. Formula (28) is accurate in the wide interval of frequencies, $0 < W\sigma/g < 75$, where the wind speed W is assigned to the level $z = 10$ m above mean water level.

4.1.2. Boundary layer parameters description

Once the input term is completely specified, all boundary layer parameters, including: the vertical wind profile, $W(z)$; friction velocity, u_*; drag coefficient, C_d; roughness height, z_0; can be estimated from the theory of dynamic boundary layer, as given below. According to the theory of Makin and Kudryavtsev (1999), the wind profile can be calculated using

$$W(z) = \frac{u_*}{0.4}\int_{z_0^v}^{z}\left[1 - \frac{I(z)}{1 + I(0)}\right]^{3/4}\mathrm{d}(\ln z), \tag{29}$$

where $I(z)$ is the function depending on 2D-spectrum of wind waves by the expression

$$I(z) = \int_{\sigma_{\min}}^{\sigma_{\max}} \mathrm{d}\sigma \oint_{\theta} \mathrm{d}\theta \left[\exp(-zk/\pi)\cos(5\pi zk)\beta\left(\frac{u_*\sigma}{g}, \theta\right) k^2 S(\sigma,\theta)|\cos(\theta)| \right]. \tag{30}$$

Here, $z_0^v \cong 0.1\frac{v}{u_*'} \cong 0.00005/W_{10}$ is the air viscosity sub-layer height; $\beta\left(\frac{u_*\sigma}{g}, \theta\right)$ is the input growing increment, given by formula (28); k is the module of the wave vector corresponding to the wave component with frequency σ. Parameter $\sigma_{\min}$ in Eq. (30) is equal to σ_{low}, and $\sigma_{\max}$ is specified by fitting ($\sigma_{\max} \cong 60$ rad/s in this model). For the frequencies higher than the upper range of the frequency interval given by (18), one can use the spectrum tail as

$$S(\sigma,\theta) \propto \sigma^{-5}\cos^2(\theta - \theta_{\text{w}}). \tag{31}$$

Estimates of u_* and $C_{\text{d}}(10)$ for the reference level $z = 10$ m are given by

$$u_* = 0.4W_{10}/J_{10}, \tag{32}$$

and

$$C_{\text{d}}(10) = [0.4/J_{10}]^2, \tag{33}$$

where $J_{10} \equiv J(10)$ is defined by the integral in the right hand side of Eq. (29). For calculation of the roughness height z_0 the logarithmic wind profile is used

$$z_0 = 10/\exp(J_{10}), \tag{34}$$

where $z_0 \equiv z_{10}$ is assigned to the standard level of 10 m.

Hence, expressions 29,30 and (32)–(34) give a complete description of the air boundary layer dependence on wind wave state. Some applications of the described above atmospheric block in a contents of wave model can be found in Polnikov et al. (2003).

4.2. *Dis*-term

The dissipation term is theoretically least investigated; therefore, there is no yet a commonly accepted parameterization. Due to crucial role of this mechanism in exchange processes at the air–sea interface, parameterization of the *Dis*-term is given below following Polnikov (1994).

4.2.1. New approach to dissipation description

We start from the well known formula for viscosity dissipation (Komen et al., 1994)

$$Dis(\sigma,\theta,S,\mathbf{W}) = \nu_{\text{T}}(\sigma,\theta,S,\mathbf{W})k^2 S(\sigma,\theta), \tag{35}$$

which is applied directly to the middle scale motions, and includes major physical phenomena of the system. Here, the function ν_{T} identifies effective viscosity due to turbulence generated by different dissipation processes, such as wave breaking, whitecapping, sprinkling, shear flows, etc. In this approach, the real origin of the turbulence is difficult to trace, because it can be attributed to all the above named phenomena simultaneously. Eq. (35) considers only the fact that turbulence is present in the upper layer. Our aim is to express the main characteristic of small-scale turbulent processes (i.e. ν_{T}) via middle-scale process parameters including wave spectrum $S(\sigma,\theta)$.

We assume that function v_T for each wave component with frequency σ and propagation direction θ, can be expressed in terms of the following wind–wave system parameters: σ, g, $\mathbf{W}$, and $S(\sigma,\theta)$. Estimating the parameter

$$\alpha = S(\sigma)\sigma^5/g^2 \cong 10^{-2}, \tag{36}$$

to be small, a general form of $v_T(\sigma,g,\mathbf{W},S)$ can be written as

$$v_T = C(\sigma,g,\mathbf{W})\sum_{n=0}^{N} v_n(\sigma,g,\mathbf{W})\alpha^n, \tag{37}$$

where coefficients v_n (with a viscosity dimension) are independent of the spectrum.

The series (37) may be restricted by a few first terms, $N \leqslant 3$ (as in Polnikov, 1994). The dimensionless fitting function $C(\sigma,g,\mathbf{W})$ can be derived considering existence of equilibrium spectral shape, $S_{eq}(\sigma,\theta)$, in the high frequency domain, $\sigma > 2.5\sigma_p$, where the spectrum shape has to satisfy the following condition

$$F|_{S=S_{eq}} = [Nl + In - Dis]|_{S=S_{eq}} \approx 0. \tag{38}$$

At this stage, functions $Nl(S)$ and $In(\sigma,g,\mathbf{W},S)$ are assumed to be known (see this section above); therefore, definition of $v_T(\sigma,g,\mathbf{W},S)$ can be done explicitly using following simplifications.

Firstly, to simplify definition of *Dis*, we exclude the term *Nl* from the condition (38). This is due to smaller contribution (<15%) of *Nl* into function *F* at the high frequency domain, comparing to other summands of the source function (see estimations of Komen et al., 1994; Efimov and Polnikov, 1991). Therefore, Eq. (38) can be replaced with

$$[In - Dis]|_{S=S_{eq}} \approx 0. \tag{39}$$

Secondly, we restrict our approximation of the total source function *F* by a third order function with respect to the wave spectrum *S*. A linear term of this function can be ascribed to function *In*, the third order one to *Nl*, and term *Dis* utilizes the second power of *S*. Note that for a numerical approximation of *F*, the linear and cubic summands of *Dis*, provided by formula (37), cannot be separated from the proper power terms in *In* and *Nl*. Therefore, one does not need to identify them, instead take into account the term $v_1(\sigma,g,\mathbf{W})$ only.

Thirdly, to obtain spectral form of the small-scale parameter, $v_1(\sigma,g,\mathbf{W})$, one can use typical turbulent theory with a semi-phenomenological closure of Reynolds stress terms. Our version of such a theory is given in Polnikov (1994).

4.2.1.1. Final specification of the dissipation term. Summarizing assumptions made above, the expression for dissipation term in deep water becomes

$$Dis(\sigma,\theta,S,\mathbf{U}) = c(\sigma,\theta,\sigma_p)\max[0.00005,\beta(\sigma,\theta,\mathbf{W})]\frac{\sigma^6}{g^2}S^2(\sigma,\theta). \tag{40}$$

Here, the wave growing parameter $\beta(\sigma,\theta,\mathbf{W})$ is given by formula (28), and the limiting value 0.00005 is introduced to describe background turbulence in the ocean upper layer. The unit-less fitting function $c(\sigma,\theta,\sigma_p)$ describes fine details of dissipation rate in the vicinity of peak frequency

σ_p and specific angular dependence of *Dis*-term. In the present version of the model, the latter function is given by

$$c(\sigma,\theta,\sigma_p) = 32\max\lfloor 0,(\sigma-0.5\sigma_p)/\sigma\rfloor T(\sigma,\theta,\sigma_p), \tag{41}$$

and

$$T(\sigma,\theta,\sigma_p) = \left\{1+4\frac{\sigma}{\sigma_p}\sin^2\left(\frac{\theta-\theta_u}{2}\right)\right\}\max[1,1-\cos(\theta-\theta_u)]. \tag{42}$$

In the angular function (42), the first factor is introduced to describe the angular dependence of *Dis* at high frequencies, and the second one does the angular dependence for opposing wind. Expressions (40)–(42) finalize description of the dissipation term, and are used for the estimation given in the next section.

5. Numerical estimation of the relative dissipation rate

5.1. Model specification

To estimate energy dissipated by wind waves, it is required to specify several numerical grids for solution of Eq. (2), and to consider the entire source function F for the selected wind wave model (described in the previous section).

5.1.1. Numerical grids

It is clear that numerical calculation of wind wave spectrum evolution has to be made at a frequency-angle numerical grid, such as the one described by expressions (18)–(20). Space–time evolution of the wave spectrum $S(\sigma,\theta)$ is considered in a rectangular $NX\times NY\,(30\times 3)$ domain. Wind is directed along OX and the grid is quadratic, $\Delta X=\Delta Y$. Initial conditions of the wave spectrum field are specified according to a problem considered. Steady-state boundary condition is assumed at one edge of the domain, $X=0$. Lateral boundary conditions (at $Y=0$ and $Y=NY\cdot\Delta Y$) changes with time according to the spectrum at the internal grid points (the so-called "open boundary conditions" which imitate an infinite shore line). Time step, Δt, is varying in a wide range depending on the given task. The first-order accurate implicit upstream numerical scheme is used to solve the evolution equation (2) for each spectral wave component $S(\sigma,\theta)$.

5.2. Numerical estimations

The main aim of calculations is to estimate energy dissipated by wind waves per unit of time of unit area. The dissipation rate is proportional to the magnitude D_E given by Eq. (14). Due to dependence of magnitude D_E on the spectral intensity, it has a wide range of variability. To normalize the value, a unit-less relative dissipation rate (RDR), D_{RE} can be introduced as

$$D_{RE} = D_E/Ef_p. \tag{43}$$

This value is as a relative part of wave energy dissipated by waves for a main wave period, $T=1/f_p$, given in units of the total wave energy. One expects that due to a small variability, values of D_{RE} could be easily tabulated and used for practical applications. Once D_{RE} is tabulated, an

estimation of D_{E} follows immediately from value for D_{RE} as far as the values of wave energy E and peak frequency f_{p} are simply defined. For a completeness of calculations, the relative input of wave energy, I_{RE} can be estimated using

$$I_{\mathrm{RE}} = \rho_{\mathrm{w}} g \int_0^{\infty} \mathrm{d}\sigma \int_0^{2\pi} \mathrm{d}\theta In(\sigma, \theta, \mathbf{W})/Ef_{\mathrm{p}}. \tag{44}$$

It is clear that D_{RE} and I_{RE} can vary depending on meteorological conditions. Therefore, the values can not be simply expressed via the local wind, **W(x)**, but they have to be computed separately for each wind field and respective boundary conditions. To understand typical variability of the values, we estimate D_{RE} and I_{RE} for two simple meteorological scenarios, including straight fetch evolution and swell decay (full description of scenarios is given in Polnikov (2005) and Efimov and Polnikov (1991).

5.2.1. Straight fetch

Problem formulation. Spatially uniform and steady state wind, $\mathbf{W}(\mathbf{x}, t) = \text{const.}$, is blowing normally to an infinite straight shore line. Initial conditions are given by uniform wave field with the JONSWAP spectral shape (Komen et al., 1994). Initial peak frequency is taken of the order of triple peak value for the fully developed waves. Wind direction, θ_{w}, and initial general direction for waves, θ_{p}, are the same: $\theta_{\mathrm{w}} = \theta_{\mathrm{p}} = 0$. "Open boundary conditions" for waves, corresponding to the case of infinite shore line, are used. The purpose of calculations is to estimate values of D_{RE} and I_{RE} for the wind wave growing scenario with different wind speed.

Resulting unit-less wave energy is introduced as

$$\widetilde{E}(\widetilde{X}) = \frac{Eg^2}{W^4}, \tag{45}$$

and dimensionless values of $D_{\mathrm{RE}}(\widetilde{X})$ and $I_{\mathrm{RE}}(\widetilde{X})$ are given by formulas (14), (43), (44), where the unit-less fetch is

$$\widetilde{X} = \frac{Xg}{W^2}. \tag{46}$$

For simplicity, all functions are considered for the steady state wave field.

Calculation results for different wind speed, $W = 10$, and 30 m/s, are presented in Figs. 3 and 4. Fig. 3 shows a good agreement of the suggested function $\widetilde{E}(\widetilde{X})$ with empirical relationships for the stable stratification case (Komen et al., 1994) for different wind speed. It means that the model is well fitted.

Analyzing the result, it is important to note that unit-less wave energy values have a very wide dynamical range, while the variability of values of $D_{\mathrm{RE}}(\widetilde{X})$ and $I_{\mathrm{RE}}(\widetilde{X})$ is quite restricted (Fig. 4). For rather long fetches, when $\widetilde{X} > 10^4$, the both curves become nearly constant:

$$D_{\mathrm{RE}}(\widetilde{X}) \approx I_{\mathrm{RE}}(\widetilde{X}) \approx 0.001. \tag{47}$$

Moreover, they have no significant dependence on the wind speed. It means that the obtained values of $D_{\mathrm{RE}}(\widetilde{X})$ and $I_{\mathrm{RE}}(\widetilde{X})$ are correct for a wide range of wind speeds. This is a very important new result which has potentially a wide range of practical applications (see next section below).

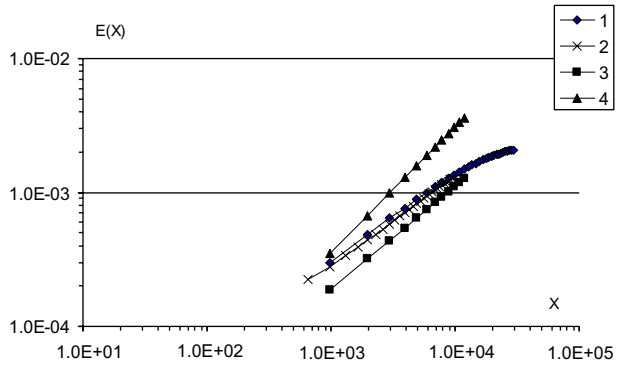

Fig. 3. Dependence $\widetilde{E}(\widetilde{X})$ for two wind speeds: 1—W=10 m/s, 2—$W = 30$ m/s. Empirical dependencies for stable (line 3) and unstable (line 4) atmospheric stratification are presented from Komen et al. (1994) as the reference curves.

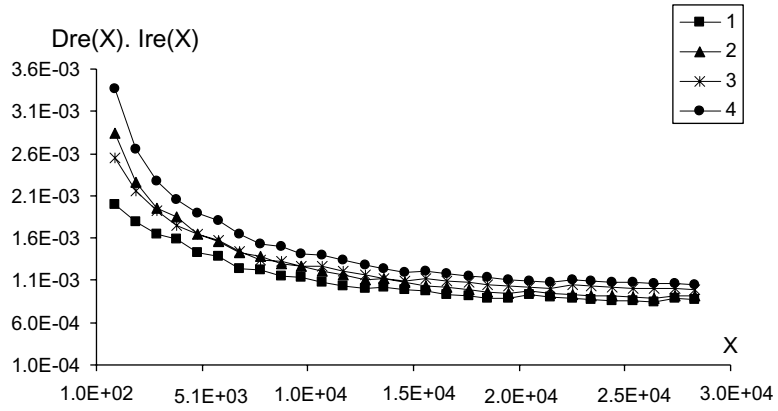

Fig. 4. Plot of unit-less values $D_{\mathrm{RE}}(\widetilde{X})$ (lines 1, 3) and $I_{\mathrm{RE}}(\widetilde{X})$ (lines 2, 4). Lines 1, 2—$W = 10$ m/s; lines 3, 4—$W = 30$ m/s.

Physical interpretation of result (47) could be the following. First of all, we may suggest with minor loss of generality that the shape of spectrum for a fully developed sea can be described by the Phillips spectrum: $S_{\mathrm{d}}(\omega) \approx \alpha_{\mathrm{p}} g^2 \omega^{-5}$ for $\omega > \omega_{\mathrm{p}}$, and $S(\omega) = 0$ for $\omega < \omega_{\mathrm{p}}$, where the peak frequency $\omega_{\mathrm{p}} \approx g/W(10)$. Then, taking into account the simplest formula of Snyder et al. (1981) for the input term $In \approx 0.3 \frac{\rho_{\mathrm{a}}}{\rho_{\mathrm{w}}} (\frac{W(10)\omega}{g} - 1)\omega S(\omega)$, one can easily find by direct integration that $I_{\mathrm{RE}} \approx \text{const.} \frac{\rho_{\mathrm{a}}}{\rho_{\mathrm{w}}} \approx 0.001$ with no dependence on the wind. Just this result is obtained by numerical calculations. It is naturally that D_{RE} is close to I_{RE} for the reason of stationary state of spectrum. That finishes the proper interpretation of result (47).[4]

[4] We acknowledge the reviewer's suggestion of this idea.

5.2.2. Swell decay test

Problem formulation. Let us assume zero wind, $W = 0$. Initial uniform wave field is characterized by the Pierson–Moscowitz spectrum (Komen et al., 1994). Initial peak frequency of swells, $f_0 \equiv f_p(0)$, is assumed at the interval 0.8–0.24 Hz. Waves at the boundary $X = 0$ are steady-state (swell producing boundary), conditions at lateral boundaries correspond to "open boundaries". Two computer runs are performed: (a) $f_0 = 0.09$ Hz, and (b) $f_0 = 0.24$ Hz.

The purpose of the test is to compare swell decay features for different initial peak frequencies. The compared values are: relative energy decay curve,

$$R(X) = E(X)/E(0), \tag{48}$$

and dimensionless values of $D_{RE}(X)$ and $I_{RE}(X)$ as functions of swell propagating distance X (Figs. 5 and 6).

As one can see from Fig. 5, the swell energy is dissipated differently for the different initial peak frequency of swell. The phenomenon was discussed extensively in Polnikov (1991, 2005). For our present study it is important to note that the relative dissipation rate D_{RE} in the case of swell decay is much more smaller (≈100 times) than in the case of wind presence. The same time, the relative rate of wind input I_{RE} becomes negative according to relationships (27), (28) and (45). This is manifested as an additional dissipation mechanism for swell. The value of I_{RE} is of the order of -4×10^{-5}, which several times greater than values D_{RE} at large distances of swell propagation (Fig. 6).

The above analysis helps to draw following conclusions. Firstly, at propagation distances of swell more than 20–40 km (which are mush smaller than typical water domains of interest) the value of D_{RE} is very small to be responsible for the energy transfer to the upper layer of water column; i.e., swells do not impact significantly exchange processes at the air–sea interface. Secondly, for the same spatial scale the relative rate of swell energy transfer into the air boundary layer is rather large, i.e., swells can change parameters of the boundary layer. Moreover, in the case of mixed wind sea (wind–waves together with swells), swells can influence the entire wind sea state. Some evidences of this phenomenon were observed in experiments (Drennan et al.,

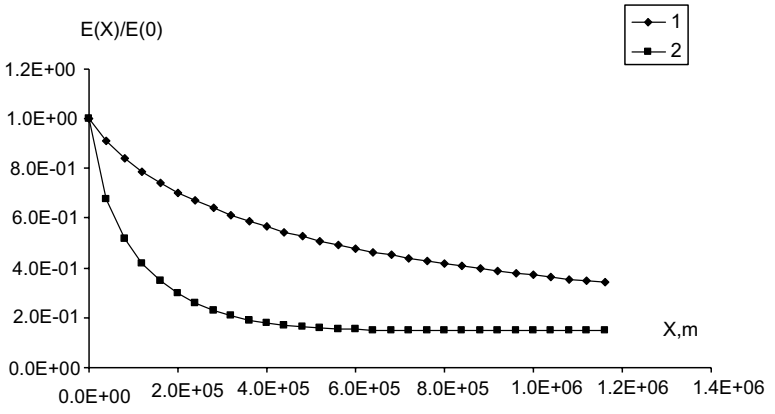

Fig. 5. Dependence of relative swell energy on the propagation distance for two initial peak frequencies: 1—$f_0 = 0.09$ Hz, 2—$f_0 = 0.24$ Hz.

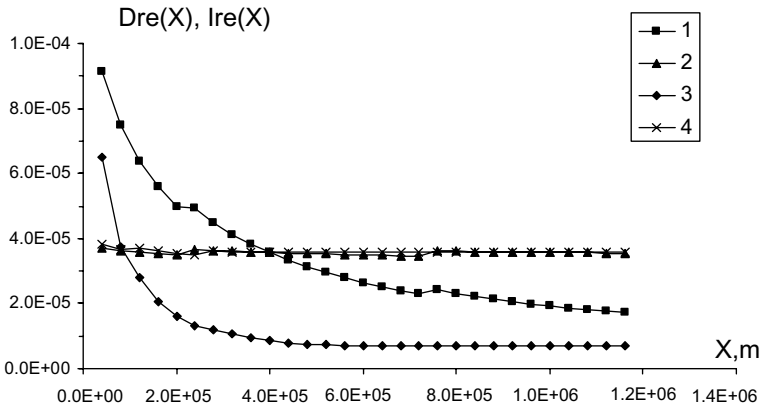

Fig. 6. Variability of unit-less values D_{RE} (lines 1, 3) and I_{RE} (lines 2, 4) with the distance of swell propagation: 1, 3—$f_0 = 0.09$ Hz; 2, 4—$f_0 = 0.24$ Hz.

1999; Grachev and Fairall, 2001). We should note that this mechanism of wave influence on the boundary layer is different from mechanism described by Makin and Kudryavtsev (1999). This new result could help to understand processes in the case of mixed wind sea, but it requires a special separate consideration.

6. Some practical applications

It is generally understood that turbulence is responsible for exchange processes in the upper layer of the water column. These may include, an air bubbles entrainment, vertical mixing of soluble and immiscible contaminants, gas and heat transfer through the surface, drift velocity formation, and others. In Section 3 it was shown that the necessary energy is provided via the wind wave dissipation mechanism. Numerical estimations of the energy supply have been completed above. In this section the theoretical estimations are utilized to elaborate results obtained earlier by Tkalich and Chan (2002a,b).

6.1. Acoustic noise dependence on the ambient wind

One of important practical problems of underwater acoustics is quantification of acoustic noise generated by air bubbles in the upper layer of the water column. Due to the phenomenon complexity, most of studies are of empirical nature (for references, see Tkalich and Chan, 2002a). Modern understanding of the phenomenon suggests that breaking waves involve air from the surface into the mixing layer, and provide energy for the bubble separation, mixing and oscillation. Oscillating bubbles are the most powerful natural sources of underwater acoustic noise. Description and prediction of the noise implies quantification of energy exchange in the chain: "wind → wind waves generation and propagation → wave breaking → bubble entrainment → bubble oscillation → acoustic energy emission". The final goal is to develop a physical model connecting the noise intensity to the local wind speed. Using estimations of the relative dissipation rate found in the previous section, the bubble acoustic noise model of Tkalich and Chan (2002a) is revisited.

In the paper it was found (under some physical assumptions) that intensity of the acoustic noise due to the bubble cloud in the upper layer, I_a, is governed by the following relationship

$$I_a = C_T R(W, H_S) \cdot (f_0/f_r)^2, \tag{49}$$

where C_T is the coefficient of theory; $R(W, H_S)$ is the radius of the bubble cloud as a function of local wind W and significant wave height H_S; (f_r/f_0) is the dimensionless oscillation frequency of bubbles having radius r; f_0 is the specific acoustic frequency. In formula (49) the linear dependence of acoustic noise intensity on the cloud radius R is of a particular interest.

In the same paper of Tkalich and Chan (2002a) it was found that the bubble cloud radius, R, is related to the dissipated wave energy as

$$R(W, H_S) = c_b c_d \frac{D_E}{Bh}. \tag{50}$$

Here, D_E is the rate of dissipated wave energy, $c_b \sim (0.3-0.5)$ is the fraction of D_E spent to the bubble cloud entrainment; $c_d \approx 0.5$ is the fraction of D_E supplied into the upper layer turbulence per unit of time and area, B is the void fraction of bubbles, and h is the characteristic depth of the bubble cloud (center of mass). Coefficient c_b is estimated from observations, c_d can be computed using (17), and to quantify values of B and h additional physical considerations and scale analysis must be employed.

By definition, magnitude of D_E can be estimated from expression (43) using dimensionless wind wave dissipation rate D_{RE}. The latter has been numerically assessed early in the paper for two simple meteorological conditions. Thus, in the case of the constant and homogeneous wind, one has

$$D_E = 0.001 E_w f_p. \tag{51}$$

This expression permits to estimate the acoustic bubble noise intensity dependence on wind in the case of constant and homogeneous wind field. Indeed, in the particular case of fully developed sea, $E_w \approx 3 \times 10^{-3} W^4 g^2$ and $f_p \approx g/W2\pi$ (Komen et al., 1994), resulting in

$$E_w(W) f_p(W) \cong 5 \times 10^{-4} W^3/g. \tag{52}$$

Omitting all coefficients independent of wind, the relationship (49) yields

$$I_a(W) \propto W^3/B(W)h(W). \tag{53}$$

Following observations we assume that value B is independent of wind. Thus, the sought dependence I_a on wind speed is defined by the expression $h(W)$. Here we have several choices, as follows.

For moderately developed waves, the following approximation is widely accepted (Tkalich and Chan, 2002a)

$$h \approx 0.35 H_S, \tag{54}$$

where H_S is the significant wave height. Using the definition $H_S = 1.4(E_w)^{1/2}$ expression (53) leads to the relationship

$$I_a \sim W. \tag{55}$$

On the other hand, in the case of fully developed sea, the characteristic depth of the bubble cloud should be correlated to the bubble cloud radius, R; therefore, assuming $h \propto R$ the Eq. (50) leads to

$$h(W) \propto W^{3/2}. \tag{56}$$

In such a case, we have

$$I_a \sim W^{3/2}. \tag{57}$$

In the case of weak wind the assumption $h = \text{const.}$ is more appropriate, therefore

$$I_a \sim W^3. \tag{58}$$

The three cases, 55,57,58, are well comparable to empirical relationships summarized in Table 1 adopted from Tkalich and Chan (2002a). It means that the physical approach used here is rather reasonable and important for a number of applications. More detailed comparison requires knowledge of real wind sea conditions, further estimation of involved experimental constants, and additional theoretical considerations. Nevertheless, one can state that the next step in understanding of the problem is done successfully.

6.2. Rate of oil film vertical mixing under breaking wind waves

Similar estimations can be executed in the case of vertical mixing of oil films, spilled on the water surface. According to Tkalich and Chan (2002b), the rate of oil entrainment from the slick to the upper mixing layer of the water column can be estimated as

$$I_o \propto c_b c_d \frac{D_E}{h}. \tag{59}$$

Here, c_b is the fraction of dissipated wave energy spent to the oil droplets entrainment, and h is the mean thickness of the mixed layer. The magnitude D_E is the dimensional wind wave dissipation rate estimated in the previous section. In the case of constant and homogeneous wind field the rate of oil mixing becomes

$$I_o \propto E_w f_p / h. \tag{60}$$

To estimate h, one can scale growth of the mixed layer thickness with the rate of wave energy dissipation as

Table 1
Observed dependence of the bubble cloud acoustic intensity on the wind speed

	Wind speed (m/s)	Acoustic intensity, I	Wave state during acoustic measurements
I	$W < 5$	0	Capillary
II	$5 < W < 10$	$\sim \left\{ \begin{matrix} 0.004W^3 - 0.049W^2 \\ +0.463W - 1.5 \end{matrix} \right\}$	Gravity-capillary
III	$10 < W < 15$		Limited duration of wave growing
IV	$W > 15$	$\sim W^{1.5}$	Fully developed sea

$$\frac{\partial h}{\partial t} \propto I_{\mathrm{o}} \propto \frac{D_{\mathrm{E}}}{h}, \tag{61}$$

leading to

$$h \propto D_{\mathrm{E}}^{1/2}. \tag{62}$$

Hence, for the nearly developed sea we obtain

$$I_{\mathrm{o}} \propto D_{\mathrm{E}}^{1/2} \propto W^{3/2}. \tag{63}$$

This relationship is in a reasonable agreement with observations (see references in Tkalich and Chan, 2002b), indicating correctness of the theoretical assumptions. Similar, the proposed approach could be applied to solve problems of gas and heat exchange at the air–sea interface and other relevant problems.

6.3. Surface boundary condition in the water circulation models

Wave energy input rate I_{E} and dissipation rate D_{E} can be utilized for the water surface boundary conditions in current circulation models. We follow Pedlosky's (1982) boundary conditions for several separate phenomena, as:

- for the horizontal shear flow, $\mathbf{U} = (u, v)$

$$\rho_{\mathrm{w}} K_t \frac{\partial \vec{U}}{\partial z} = \vec{\tau}, \tag{64}$$

- for the turbulent kinetic energy, k:

$$k = \frac{\tau}{(c_\mu^0)^2} \left(\text{or alternatively} \frac{\partial k}{\partial z} = 0 \right), \tag{65}$$

- for the rate of turbulent kinetic energy dissipation, $\varepsilon = (c_\mu^0)^3 \frac{k^{3/2}}{L}$,

$$v_\varepsilon \frac{\partial \varepsilon}{\partial \tilde{z}} = (c_\mu^0)^3 \frac{k^{3/2}}{\kappa(\tilde{z} + z_0)^2}. \tag{66}$$

Here, τ, K_t, c_μ^0, L, z_0, and others are specific theoretical parameters of the system under consideration. At present time the simplest information on wind stress, τ, and water surface roughness, z_0, is used traditionally. However, following derivations given in Sections 3 and 4 of this paper, it is clear that the surface wind stress in relationships 64, 65 can be modified according to formulae 11, 32, 33. Proper estimate of z_0 should be done in the condition (66), as well. Moreover, in expression (64) one should use a turbulent part of the wind stress depending on the rate I_{E} while in (65) does the wave part of the stress defining by the rate D_{E}. Eventually, a model for the current circulation could improve accuracy by coupling with a wind wave model, in (at least simple) parametric form.

7. Conclusions

In this paper the wind energy and momentum exchange under breaking wind waves are analyzed. The considered forces are part of intermediate scale motions at the air–sea interface. It is shown that the energy input phenomena are controlling the boundary layer state, while wind wave dissipation processes define state of the upper layer of the water column. To demonstrate role of wind waves in the energy exchange, a new model of Polnikov (2005) is used. In the model, traditional approach for the wave input mechanism is enforced by the dynamic boundary layer model (Makin and Kudryavtsev, 1999), and the dissipation part of the source term is represented using theory of Polnikov (1994).

Mathematical definitions for the relative wave energy input rate, I_{RE} and dissipation rate, D_{RE} are suggested, and numerical estimations of the values are completed for two simple meteorological scenarios: wave growth and swell decay. These estimations show that in the case of fully developed sea, the relative characteristics I_{RE} and D_{RE} are nearly independent of the wind, namely,

$$I_{\mathrm{RE}} \cong D_{\mathrm{RE}} \cong 0.001. \tag{67}$$

In the case of swell decay, the values are

$$D_{\mathrm{RE}} \cong (1\text{–}2) \times 10^{-5}; \quad I_{\mathrm{RE}} \cong -4 \times 10^{-5}. \tag{68}$$

Estimation (67) permitted derivation of theoretical dependences of acoustic noise intensity on the wind speed for several stages of wind waves development, as well as estimation of oil film mixing rate under breaking waves. In the both cases the theoretical estimations are in a reasonable correspondence with observations. This lay a ground for a wide use of the method to more complicated wave fields.

The result (68) addresses phenomenon of swell influence on parameters of air boundary layer. Taking into account recent observations by Drennan et al. (1999); Grachev and Fairall (2001), there is a high potential for practical use of the theoretical result.

Some applications of the theory may improve accuracy of current circulation modeling. The suggested approach initiates more accurate description of exchange processes at the air–sea interface.

Acknowledgements

This work was initiated by the Tropical Marine Science Institute, and was funded by the Eastern Europe Research Scientist and Student Exchange program of National University of Singapore. Partially it was supported by the Russian Foundation for Basic Research, project no. 04-05-64650. We are thankful to reviewers for numerous useful remarks and suggestions.

References

Banner, M. (Ed.), 1999. Proceedings of the Symposium on the Wind Driven Air–Sea Interface. The University of New South Wales, Sydney, Australia, 452 pp.

Chalikov, D.V., 1980. Numerical simulation of the boundary layer above waves. Boundary Layer Meteorol. 34, 63–98.

Chalikov, D.V., Belevich, M.Y., 1993. One-dimensional theory of the wave boundary layer. Boundary Layer Meteorol. 63, 65–93.

Donelan, M. (Ed.), 1994. Proceedings of the Symposium on the Wind Driven Air–Sea Interface. The University of Marseilles, France, 550 pp.

Drennan, W.M., Graber, H.C., Donelan, M.A., 1999. Evidence for the effect of swell and unsteady winds on marune wind stress. J. Phys. Oceanogr. 29, 1853–1864.

Efimov, V.V., Polnikov, V.G., 1991. Numerical Modeling of Wind Waves. Kyev. "Naukova dumka" Publishing House, 240 pp. (in Russian).

Grachev, A.A., Fairall, C.W., 2001. Upward momentum transfer in the marine boundary layer. J. Phys. Oceanogr. 31, 1698–1711.

Hasselmann, K., 1962. On the non-linear energy transfer in a gravity wave spectrum. Part 1. General theory. J. Fluid. Mech. 12, 481–500.

Hasselmann, S., Hasselmann, K., Allender, K.J., Barnett, T.P., 1985. Computations and parameterizations of the nonlinear energy transfer in a gravity-wave spectrum. Part II. J. Phys. Oceanogr. 15, 1378–1391.

Kitaigorodskii, A., Lumley, J.L., 1983. Wave–turbulence interaction in the upper layer. Part 1. J. Phys. Oceanogr. 13, 1977–1987.

Komen, G., Cavaleri, L., Donelan, M., et al., 1994. Dynamics and Modelling of Ocean Waves. Cambridge University Press, 532.

Makin, V.K., Kudryavtsev, V.N., 1999. Coupled sea surface-atmosphere model. Part 1: Wind over waves coupling. J. Geophys. Res. C104, 7613–7623.

Miles, J.W., 1957. On the generation of surface waves by shear flows. Part 1. J. Fluid Mech. 3, 185–204.

Monin, A.S., Yaglom, A.M., 1965. Statistical Hydromechanics. "Nauka" Publishing House, Moscow, 640 pp. (in Russian).

Pedlosky, J., 1982. Geophysical Fluid Dynamics. Springer-Verlag, NY, 350.

Phillips, O.M., 1957. On the generation of wind waves by turbulent wind. J. Fluid Mech. 2, 417–445.

Phillips, O.M., 1977. Dynamics of the Upper Ocean, Second ed. Cambridge University Press, 261 pp.

Plant, W.J., 1982. A relationship between wind stress and wave slope. J. Geophys. Res. 87, 1961–1967.

Polnikov, V.G., 1994. On description of wind-wave energy dissipation function. In: Proceedings of the Air–Sea Interface Symposium. Marseilles, France, pp. 227–282.

Polnikov, V.G., 1991. A third generation spectral model for wind waves. Izvestiya, Atm. Ocean. Phys. 27, 615–623 (English transl.).

Polnikov, V.G., Farina, L., 2002. On the problem of optimal approximation of the four-wave kinetic integral. Nonlinear Process. Geophys. 9, 497–512.

Polnikov, V.G., 2003. The choice of optimal discrete interaction approximation to the kinetic integral for ocean waves. Nonlinear Process. Geophys. 10, 1–10.

Polnikov, V.G., Yu, A., Volkov, F.A., Pogarskii, F.A., 2003. Interpretation of variations in the characteristics of the atmospheric boundary layer with a numerical model. Izvestiya, Atm. Ocean. Phys. 39, 369–379 (English transl.).

Polnikov, V.G., 2005. Wind wave model with optimized source function. Izvestiya, Atm. Ocean. Phys. 41, #5 (in press).

Qiao, F., Yuan, Y., Yang, Y., et al., 2004. Wave-induced mixing in the upper ocean. Distribution and application to a global ocean circulation model. Geophys. Res. Lett. 31, L11303, doi: 10.1029/2004/GL019824.

Snyder, R.L., Dobson, F.W., Elliott, J.A., Long, R.B., 1981. Array measurements of atmospheric pressure fluctuations above surface gravity waves. J. Fluid Mech. 102, 1–59.

Tolman, H.L., Chalikov, D.V., 1996. Source terms in a third generation wind wave model. J. Phys. Oceanogr. 26, 2497–2518.

Tkalich, P., Chan, E.S., 2002a. Breaking wind waves as a source of ambient noise. J. Acoust. Soc. Am. 112, 456–483.

Tkalich, P., Chan, E.S., 2002b. Vertical mixing of oil droplets by breaking waves. Marine Pollut. Bull. 44, 1219–1229.

Yan, L., 1987. An improved wind input source term for third generation ocean wave modeling. Royal Dutch Meteorological Institute, Report no. 87-8, 27 pp.